



## Adsorbents synthesized from dewatered oily sludge and their adsorption of reactive brilliant red X-3B in aqueous solution

Hao Guo<sup>a</sup>, Hai Lin<sup>b</sup>, Ying Li<sup>c</sup>, Xinliang Li<sup>d</sup>, Suping Feng<sup>a,\*</sup>, Ying Zhu<sup>e</sup>

<sup>a</sup>School of Environmental Science and Engineering, Shandong University, Jinan 250100, P.R. China, email: [gaokaobuaa@126.com](mailto:gaokaobuaa@126.com) (H. Guo), Tel./Fax: +86 531 88362819; email: [fengsuping@sdu.edu.cn](mailto:fengsuping@sdu.edu.cn) (S. Feng)

<sup>b</sup>Department of Landscape Architecture, Shandong Agriculture and Engineering University, Dezhou 251100, P.R. China, email: [2560412984@qq.com](mailto:2560412984@qq.com)

<sup>c</sup>Department of Spectrophotometry, CNGC Institute 53, Jinan 250032, P.R. China, email: [93340364@qq.com](mailto:93340364@qq.com)

<sup>d</sup>Safety and Environmental Protection Division of the Sixth Oil Recovery Plant of Zhongyuan Oilfield, Heze 274511, P.R. China, email: [zyxinliang@163.com](mailto:zyxinliang@163.com)

<sup>e</sup>New Materials Research Institute of Shandong Academy of Sciences, Jinan 250014, P.R. China, email: [25411102@qq.com](mailto:25411102@qq.com)

Received 26 April 2015; Accepted 30 January 2016

### ABSTRACT

Oily sludge was first dewatered using Fenton's reagent and sawdust, and was then made into adsorbents. These lab-made adsorbents were applied to adsorb the reactive brilliant red X-3B dye in liquid phase. The adsorbent was activated at 800 °C for 45 min in an inert atmosphere after activation for 24 h by ZnCl<sub>2</sub> at 40 wt%. Results show that the adsorbent has a maximum apparent surface area of 183 m<sup>2</sup> g<sup>-1</sup> and total volume of 0.19 cm<sup>3</sup> g<sup>-1</sup>. The results of the kinetic and isothermal studies show that the adsorbent fits the pseudo-second order and Langmuir models, respectively. Moreover, the adsorption is confirmed to be an endothermic process. The adsorbent achieved a maximum equilibrium adsorption capacity of 67.72 mg g<sup>-1</sup> at 30 °C with an equilibrium time of 8 h. A total of 8 metals, including heavy metals, were found in the raw material, and most of them, except for Fe, can hardly be dissolved into the liquid after adsorption. Although the adsorption capacity is lower than that of common commercial-activated carbon, the lab-made adsorbent has the advantages of low cost and low adsorption equilibrium time.

*Keywords:* Oily sludge; Adsorbent; X-3B; Adsorption; Heavy metal

### 1. Introduction

Activated carbon (AC) is a type of adsorbent produced from a variety of carbonaceous source materials. Given its porous structure and high surface area, it is widely used to remove organic compounds and other pollutants such as heavy metal ions in water

and air. Some ACs can also be used as catalysts or catalyst support in some catalytic processes [1].

The first ACs were mostly made from biomass materials, such as maize cobs, rice husks, and sunflower seed hulls [2]. Some experts have devoted themselves to researching materials that can be made into ACs, such as dewatered sewage sludge [3,4] and the sludge of drinking water treatment plants [5]. The adsorption effect of ACs made from above-mentioned

\*Corresponding author.

materials is usually combined with other carbonaceous sources, which are favorable for their low cost.

Very few studies thus far have focused on transforming oily sludge into adsorbent materials to utilize this byproduct generated from petroleum and other related industries.

The world oil refinery industries can produce more than 60 million tons of oily sludge, and approximately 1 billion tons of this hazardous waste was accumulated worldwide in 2012 [6].

Oily sludge usually contains 5–86.2 wt% of total petroleum hydrocarbon (TPH) by mass, more frequently in the range of 15–50 wt%, and can have a moisture content of more than 80 wt%, even reaches to 95 wt%, whereas the solid content only has a moisture content of 5–46 wt% [7].

Oily sludge can cause enormous harm to the environment and human health [7,8]. Numerous organic compounds, such as polycyclic aromatic hydrocarbons and polychlorinated dibenzodioxins, are present in oily sludge, especially in dewatered oily sludge [7,9–11].

Given its remarkable TPH content, oily sludge can be used for recycling energy and other applications. Many experts have noted the potential use of oily sludge and have exerted great research efforts in recent years. Pinheiro and Holanda [12] in Brazil made floor tiles by mixing 5 wt% with kaolin and found that the new product achieved the technical characteristics of porcelain floor tiles. Xu et al. [13] added oily sludge to coal–water slurry to improve its rheological property and obtained desirable coal–oily-sludge slurry, which can be used for syngas production. However, the multipurpose utility of oily sludge is still in the early stages, given the attention of most researchers to the dewatering of such waste [7,8,14]. Oily sludge has huge potential in resource recovery and comprehensive utilization.

At present, the wastewater discharged from the dyeing and printing industry, which contains plenty of dyes, has caused tremendous environmental and ecological problems, especially the azo dyes, such as reactive brilliant red X-3B dye (X-3B) [15]. Although several experts have made great efforts to promote the biodegradation of such dye [16–19], X-3B is a stable dye that is not easily to be degraded. Thus, adsorption of this dye may be an effective way of treating the effluent produced by the dyeing and printing industry. Some researchers have investigated the capacity of many kinds of adsorbents on adsorbing X-3B. Zhang et al. [15] used three types of layered double hydroxides to study the adsorption process of X-3B. Wu et al. [20] introduced organic and carbon aerogels for the adsorption of X-3B. However, oily sludge has not been considered in removing X-3B. In our experiment, the

adsorbent made from oily sludge and sawdust performs very well in adsorbing the azo dye.

The aim of this study is to reuse the oily sludge dewatered by a combination of Fenton's reagent and sawdust in our previous study [21]. The adsorbent made from dewatered oily sludge is also used to remove organic pollutants in wastewater to harness environmental and economic benefits.

## 2. Experimental

### 2.1. Materials and reagents

Oily sludge was obtained from the Sixth Oil Exploiting Plant of Zhongyuan Oil Field located in Dongming County, Shandong Province, China, and it was stored in a refrigerator at 4°C for less than 2 weeks to maintain the stability of its properties. The characteristics of the raw oily sludge are listed in Table 1. The pine sawdust was collected from Huangtai Furniture Market northeast of Jinan, Shandong Province, China. The sawdust was first milled into fine particles with grain sizes of no more than 0.267 mm, and then dried in an oven at 80°C for 4 h before use.

The raw oily sludge was first treated with Fenton's reagent and then mixed with the sawdust. The mixture was then filtered by a vacuum pump for dewatering, following a previously described procedure [21]. The filter cake was then dried in an oven at 105°C and then ground into powder before use, with the proportion of oily sludge and sawdust equal to 2:1 in dry mass. The X-3B was purchased from Eighth Dyestuffs Co., Ltd, Shanghai, China, and was used with no further purification. The chemical structure of X-3B is shown in Fig. 1 [22]. The zinc chloride (analytical grade) used as activator was obtained from Tianjin Guangcheng Chemical Reagent Co., Ltd, China and was used with no further purification.

### 2.2. Preparation of adsorbents

First, the dewatered oily sludge mixed with sawdust [21] was dried in a drying oven and milled into fine powder. A certain amount of powder was then

Table 1  
The characteristics of the raw oily sludge

Parameters	Unit	Value
pH	–	7.40
Solids content	%	6.56
Moisture content	%	88.11
Oily content	%	5.33

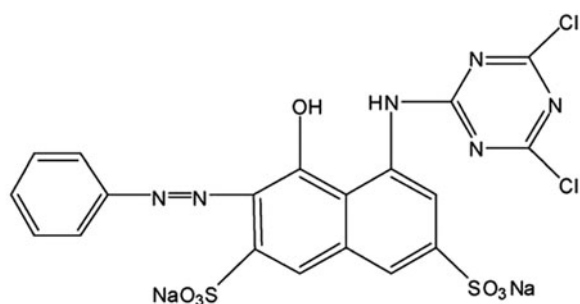


Fig. 1. The chemical structure of X-3B dye [22].

thoroughly immersed in some zinc chloride solution for 24 h. The mass of zinc chloride was set to be 40% of the powder mixture.

Second, the immersed mixture was placed in a muffle furnace (Nabertherm, Germany) and heated to 700 or 800°C for 45 min at a rate of 10°C min<sup>-1</sup>. The furnace was then cooled to ambient temperature. The N<sub>2</sub> flow was set to 5 cm<sup>3</sup> s<sup>-1</sup> to create an inert atmosphere during the whole process. The products were milled into fine powder with grain sizes of no more than 0.178 mm and were washed in deionized water. When the rinse water was neutral, the adsorbents were dried at 105°C for 24 h and stored under dry conditions for future use.

In the following experiment, we named the adsorbents carbonized in 700 and 800°C were labeled for No. 1 and No. 2, respectively, for convenience.

### 2.3. Characterization of adsorbents

The surface properties of the lab-made adsorbents were characterized using automated surface area and pore size (JW-BK122W, China) under N<sub>2</sub> adsorption/desorption isotherms at 133 Pa and 77 K. The Brunauer–Emmett–Teller (BET) surface area ( $S_{\text{BET}}$ ) was determined by the BET equation, and the pore size distribution was determined by the density functional theory method. The total volumes ( $V_{\text{tot}}$ ) and the mean pore sizes ( $D_p$ ) were calculated using the Barrett–Joyner–Halenda method. The microspore area ( $S_{\text{mic}}$ ) and microspore volume ( $V_{\text{mic}}$ ) were determined using the  $t$ -plot method. The external volume ( $V_{\text{ext}}$ ) was estimated by deducting  $V_{\text{mic}}$  from  $V_{\text{tot}}$  and the external area ( $S_{\text{ext}}$ ) was evaluated by deducting  $S_{\text{mic}}$  from  $S_{\text{tot}}$  [23]. Scanning electron microscopy (SEM, Hitachi S-520, Japan) was used to detect the surface morphologies of the selected adsorbents. The surface functional groups of the selected adsorbents were detected using a Fourier transform infrared spectrometer (FTIR) (Fourier-380FTIR, USA), with wavenum-

bers ranging from 4,000 to 400 cm<sup>-1</sup> and at a resolution of 2 cm<sup>-1</sup>. To obtain thermogravimetric analysis (TGA) and differential scanning calorimetry (DSC) curves, SDT-Q600 (USA) equipment was used. The sample consisted of compounds of dewatered oily sludge, sawdust, and ZnCl<sub>2</sub>. It was heated at a rate of 10°C min<sup>-1</sup> between 40 and 800°C under N<sub>2</sub> atmosphere. Inductively coupled plasma was introduced to detect the related heavy metals and other elements contained in the raw material and liquid obtained after adsorption.

### 2.4. Adsorption experiments

A certain amount of lab-made adsorbents and a certain volume of X-3B solution were placed into conical flasks with cover. These flasks were then shaken in a shaking operating at 150 rpm for a pre-defined time. The concentrations of X-3B after adsorption and filtration were evaluated using a V-5100 spectrophotometer (METASH, China) at a wavelength of 538 nm which corresponds to the maximum of absorbance [20]. The final concentration of the solution was then determined from the calibration curve.

The dye adsorption capacity at equilibrium,  $q_e$  (mg g<sup>-1</sup>), can be calculated using the following equation [3]:

$$q_e = \frac{(C_0 - C_e)V}{m} \quad (1)$$

where  $C_0$  (mg L<sup>-1</sup>) is the initial X-3B concentration in liquid phase,  $C_e$  (mg L<sup>-1</sup>) is the X-3B concentration in liquid phase at equilibrium,  $V$  (L) is the total volume of X-3B solution and  $m$  (g) is the mass of the adsorbent.

Two sequential types of assays were performed according to the following conditions.

#### 2.4.1. Kinetic assays

The kinetic studies were conducted using 0.05 g of adsorbent for 50 cm<sup>3</sup> of X-3B solution, with several samples collected between 0 min and 24 h.

#### 2.4.2. Isothermal assays

The isothermal studies were conducted by keeping the adsorbent dose (0.05 g) constant and by varying the X-3B concentrations (from 50 to 110 mg L<sup>-1</sup> with a 10 mg L<sup>-1</sup> disparity every sample solution). After stirring, until the adsorption equilibrium was reached

(i.e. the time obtained through kinetic assays), the concentration of X-3B remaining in solution ( $C_e$ ) was determined, and the uptake ( $q_e$ ) was calculated using Eq. (1).

The kinetic assays were conducted at 20°C, and the isothermal assays were conducted at 10, 20, and 30°C.

### 3. Results and discussion

#### 3.1. Characteristics of selected adsorbents

##### 3.1.1. Textural structure

The textural parameters of adsorbents No. 1 and No. 2 are shown in Table 2. The  $N_2$  adsorption/desorption isotherms and pore size distributions are shown in Figs. 2 and 3. As Table 2 and Figs. 2 and 3 show, the activated temperature increases, and all the textural parameters except for  $D_p$  also increase. For example, as the activated temperature was increased from 700 to 800°C, the  $S_{mic}$  increases from 132.21 to 143.66  $m^2 g^{-1}$ , although the proportion decreases from 96.1 to 78.3%. The  $V_{mic}$  also exhibits the same trend as the  $S_{mic}$ , whereas the  $S_{ext}$  and  $V_{ext}$  of adsorbents No. 1 and No. 2 exhibit the opposite trend. As the temperature increases, the  $D_p$  tend to be smaller which may lead to a larger surface area. A higher temperature is therefore beneficial to the surface area and volume development, especially the  $S_{ext}$  and  $V_{ext}$ .

##### 3.1.2. SEM analysis

The SEM micrographs (10,000×) of the two kinds of adsorbents are shown in Figs. 4a and 4b. Adsorbent No. 2 which was activated at 800°C has better developed pore structures than that activated at 700°C. Moreover, the pores on the surface of No. 1 are more asymmetrical than those of No. 2. Thus, we can conclude that a higher temperature favors pore development.

##### 3.1.3. FTIR analysis

The FTIR analysis (Fig. 5) shows the characteristic bands of adsorbents No. 1 and No. 2. These two kinds

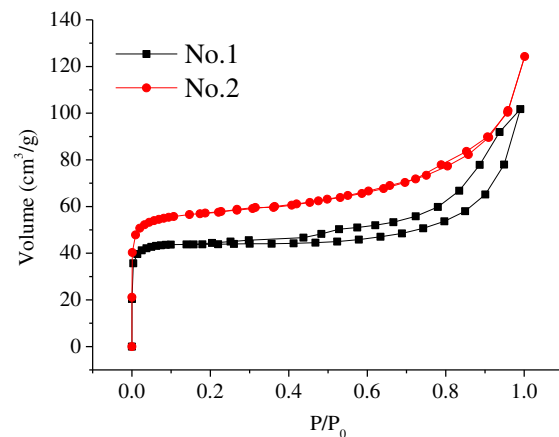


Fig. 2. The adsorption–desorption isotherms of  $N_2$  at 77 K for adsorbent No. 1 and No. 2.

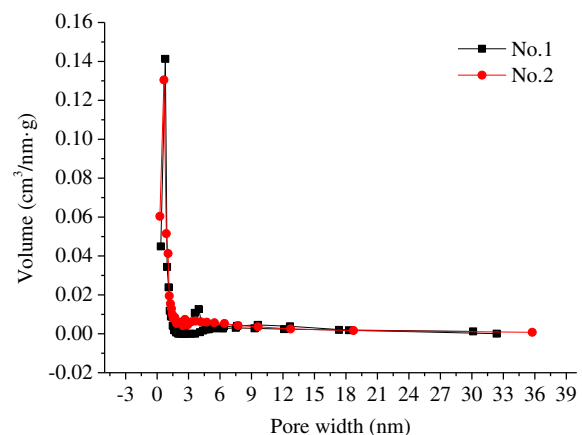


Fig. 3. Pore size distributions of adsorbent No. 1 and No. 2.

of adsorbents present similar peaks. The peak at approximately 976  $cm^{-1}$  corresponds to sulfate salts, whereas the band at approximately 908  $cm^{-1}$  is attributed to clathrate which may consist of copper and sulfate, whose carbonate stretching is at the peak of 867  $cm^{-1}$ . The last band at 575  $cm^{-1}$  is attributed to manganese oxide or chromic oxide, given that these elements exist in raw oily sludge. A large proportion

Table 2  
Porous structure parameters of the two kinds of lab-made adsorbent

No.	$S_{BET}$ ( $m^2 g^{-1}$ )	$S_{mic}$ ( $m^2 g^{-1}$ )	%	$S_{ext}$ ( $m^2 g^{-1}$ )	%	$V_{tot}$ ( $cm^3 g^{-1}$ )	$V_{mic}$ ( $cm^3 g^{-1}$ )	%	$V_{ext}$ ( $cm^3 g^{-1}$ )	%	$D_p$ (nm)
1	137.58	132.21	96.1	5.37	3.9	0.157	0.065	41.4	0.092	58.6	4.58
2	183.55	143.66	78.3	39.89	21.7	0.19	0.07	36.8	0.12	63.2	4.19

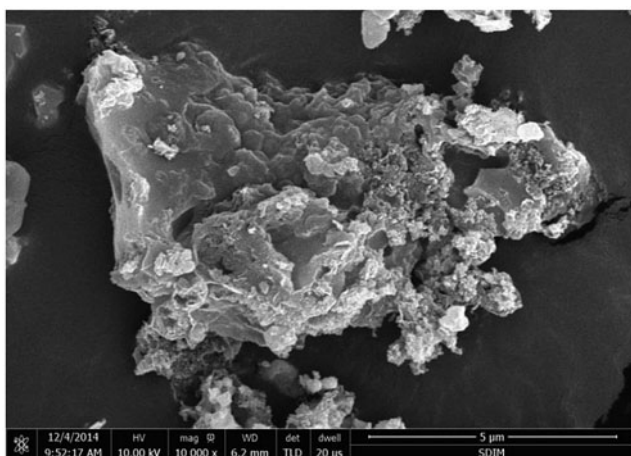


Fig. 4a. SEM micrographs of lab-made adsorbents No. 1.

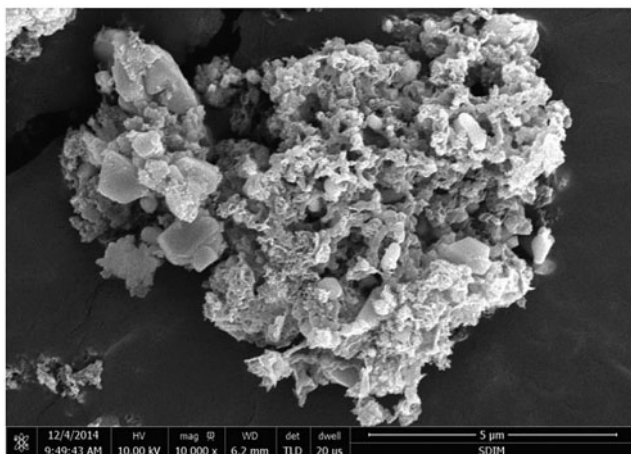


Fig. 4b. SEM micrographs of lab-made adsorbents No. 2.

of organic compounds evidently decompose after being carbonized at high temperatures and inert atmosphere, leaving only mineral salt, elemental carbon, and ash.

### 3.1.4. TGA analysis

The thermal analysis of the raw material is shown in Fig. 6. The TGA plot indicates three mass loss stages in the whole process. The first stage occurred from 21.10 to 162.37°C with a mass loss of 6.979%, which may be due to the evaporation of moisture. The following stage ranges from 162.37 to 354.09°C with a mass loss of 23.96%, which indicates the decomposition of certain organics. The last stage, as can be seen in Fig. 6, involves the pyrolysis of the remaining organics and carbonate salts, these compounds occupy 21.02% of the total mass. The TGA result indicates that the suitable activated temperature of the dewatered oily sludge is approximately 800°C, which is in accordance with the conclusion.

### 3.2. Kinetics study

The kinetics is important, because it can facilitate understanding of the adsorption dynamics in terms of the order of the rate constant [24,25]. The three commonly used models—the pseudo-first order, pseudo-second order, and intra-particle diffusion models—are applied to fit the experimental data. The pseudo-first order, pseudo-second order, and intra-particle diffusion equations are as follows [3,23]:

$$\ln(q_e - q_t) = \ln q_e - k_1 t \quad (2)$$

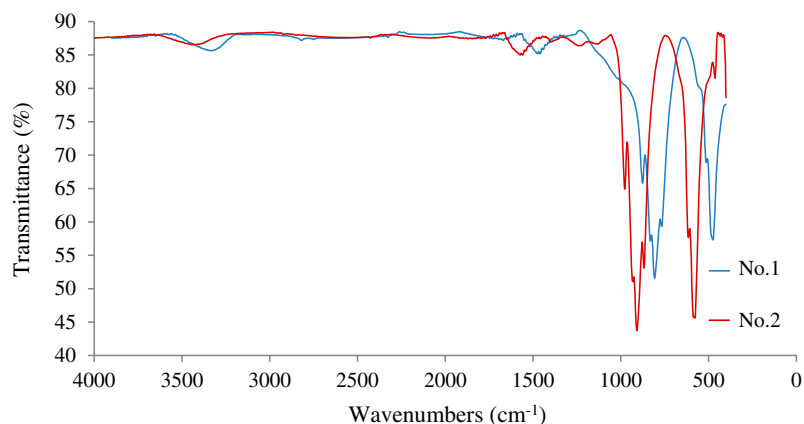


Fig. 5. FTIR spectrums of adsorbents No. 1 and No. 2.

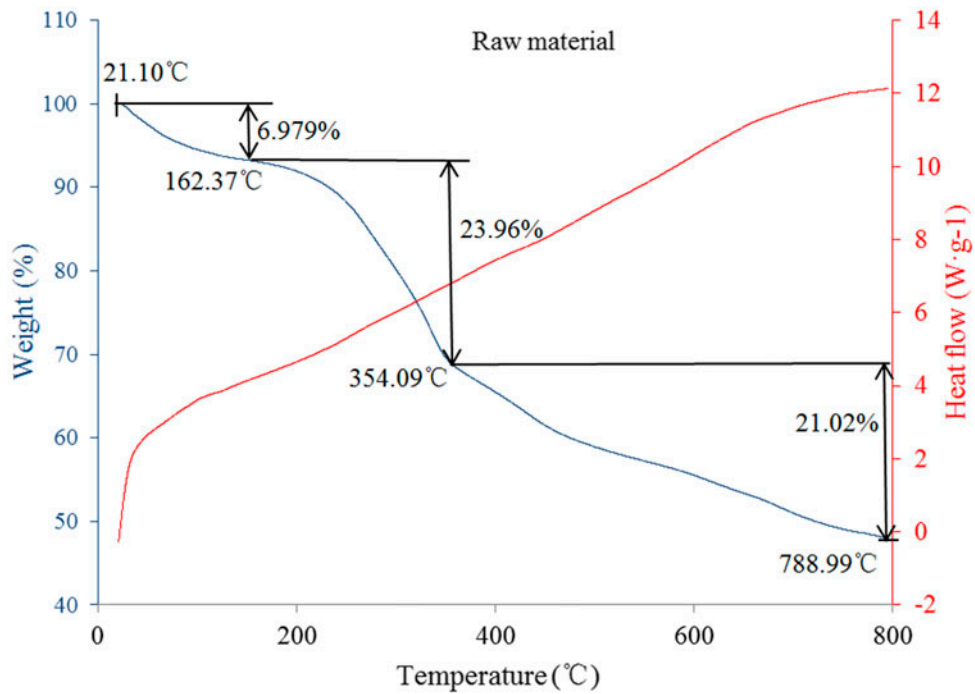


Fig. 6. DSC-TGA analysis graph of raw material.

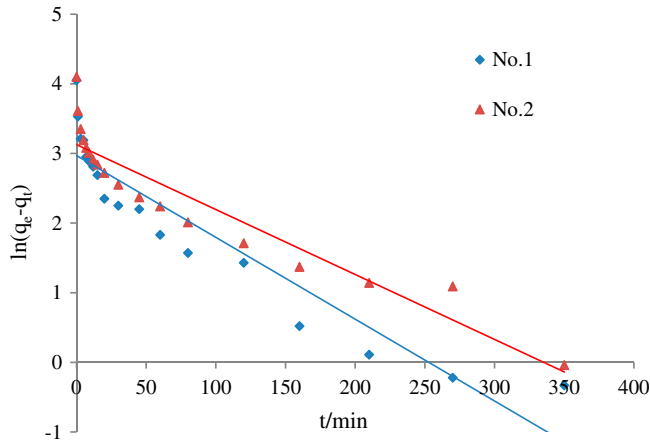


Fig. 7a. Pseudo-first-order kinetics fitting curve of X-3B on adsorbents No. 1 and No. 2 (initial concentration of X-3B is 80 mg L<sup>-1</sup>, the operation temperature is 20°C, and the assay duration is 24 h).

$$\frac{t}{q_t} = \frac{1}{k_2 q_e^2} + \frac{t}{q_e} \quad (3)$$

$$q_t = k_p t^{0.5} + C \quad (4)$$

where  $q_e$  (mg g<sup>-1</sup>) and  $q_t$  (mg g<sup>-1</sup>) are the amounts of X-3B adsorbed at equilibrium and at any time  $t$ ,

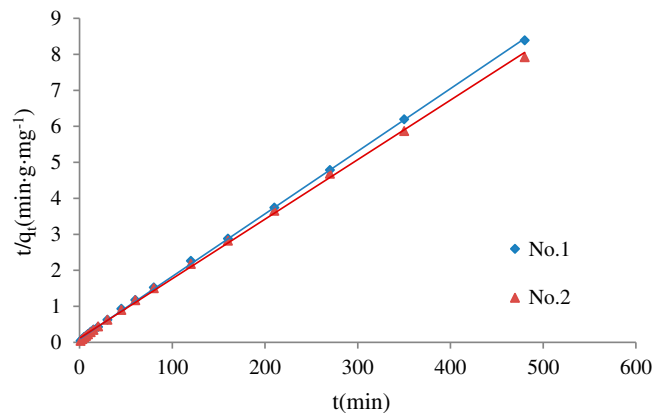


Fig. 7b. Pseudo-second-order kinetics fitting curve of X-3B on adsorbents No. 1 and No. 2 (initial concentration of X-3B is 80 mg L<sup>-1</sup>, the operating temperature is 20°C, and the assay duration is 24 h).

respectively;  $k_1$  (min<sup>-1</sup>) is the pseudo-first-order rate constant;  $k_2$  (g mg<sup>-1</sup> min<sup>-1</sup>) is the rate constant of the pseudo-second-order, and  $k_p$  (mg g<sup>-1</sup> min<sup>-0.5</sup>) is the adsorption rate constant of the intra-particle diffusion.

When we fit the adsorption kinetics data obtained in the initial concentration of 80 mg L<sup>-1</sup> of X-3B are fitted with the three above-motioed kinetics models, the linear fitting curve and fitting equation can be

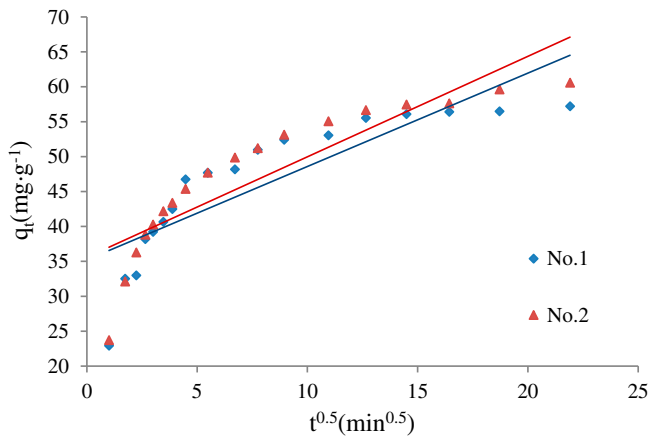


Fig. 7c. Intra-particle diffusion fitting curve of X-3B on adsorbents No. 1 and No. 2 (initial concentration of X-3B is 80 mg L<sup>-1</sup>, the operation temperature is 20°C, and the assay duration is 24 h).

obtained. The equation parameters can also be calculated through Eqs. (2)–(4). The results are shown in Figs. 7a–7c and Table 3.

Figs. 7a–7c and Table 3 show that the pseudo-second order model can fit the experimental data better because the correlation coefficients values (*R*<sup>2</sup>) of adsorbents No. 1 (0.9997) and No. 2 (0.9991) are greater than those of other models.

The pseudo-second order model assumes that the adsorption is a pseudo chemical process and considers the adsorption mechanism as the limiting factor, rather than the resistance of mass transfer inside

granules [3]. Our experimental result is in agreement with some previous studies that focus on activated sludge [26,27], which indicates that the adsorption of X-3B into adsorbents made from oily sludge and sawdust refers to the adsorption process of external liquid film diffusion, surface adsorption, and so on. In addition, the maximum adsorption capacity obtained in the experiment is close to that calculated by the model, further verifying the above conclusion.

### 3.3. Adsorption isotherms

In this study, two main isotherm models—Langmuir and Freundlich models—were used to describe the characteristics of adsorption at equilibrium.

The Langmuir isothermal model assumes that adsorption is a chemical process and that one adsorption site can adsorb only one molecule adsorbate. This model is mainly used to describe single molecular layer adsorption [28]. The Langmuir model is expressed as follows:

$$\frac{C_e}{q_e} = \frac{1}{bQ_m} + \frac{C_e}{Q_m} \tag{5}$$

where *C<sub>e</sub>* is the equilibrium concentration (mg L<sup>-1</sup>), *b* is the Langmuir constant (L mg<sup>-1</sup>), and *Q<sub>m</sub>* is the saturated absorption capacity (mg g<sup>-1</sup>).

Unlike the Langmuir isothermal equation, the Freundlich isothermal adsorption equation is only an

Table 3

Parameters of kinetic models for the adsorption of X-3B onto adsorbents No. 1 and No. 2 at an initial concentration of 80 mg L<sup>-1</sup>

Kinetic models	Parameters	Initial X-3B concentration: 80 mg L <sup>-1</sup>	
		Adsorbent No. 1	Adsorbent No. 2
Pseudo-first-order	<i>q<sub>e,exp</sub></i> (mg g <sup>-1</sup> )	57.21	60.58
	<i>q<sub>e,cal</sub></i> (mg g <sup>-1</sup> )	19.47	22.79
	<i>k<sub>1</sub></i> (min <sup>-1</sup> )	0.0117	0.0093
	<i>R</i> <sup>2</sup>	0.8775	0.8799
Pseudo-second-order	<i>q<sub>e,exp</sub></i> (mg g <sup>-1</sup> )	57.21	60.58
	<i>q<sub>e,cal</sub></i> (mg g <sup>-1</sup> )	57.47	60.61
	<i>k<sub>2</sub></i> (g mg <sup>-1</sup> min <sup>-1</sup> )	0.0033	0.0024
	<i>R</i> <sup>2</sup>	0.9997	0.9991
Intra-particle diffusion	<i>q<sub>e,exp</sub></i> (mg g <sup>-1</sup> )	57.21	60.58
	<i>q<sub>e,cal</sub></i> (mg g <sup>-1</sup> )	60.67	62.56
	<i>k<sub>p</sub></i> (g mg <sup>-1</sup> min <sup>-1</sup> )	1.3374	1.4389
	<i>R</i> <sup>2</sup>	0.7248	0.7816

Notes: *q<sub>e,exp</sub>* and *q<sub>e,cal</sub>* represent the adsorption capacity obtained in experiment and calculated by model, respectively.

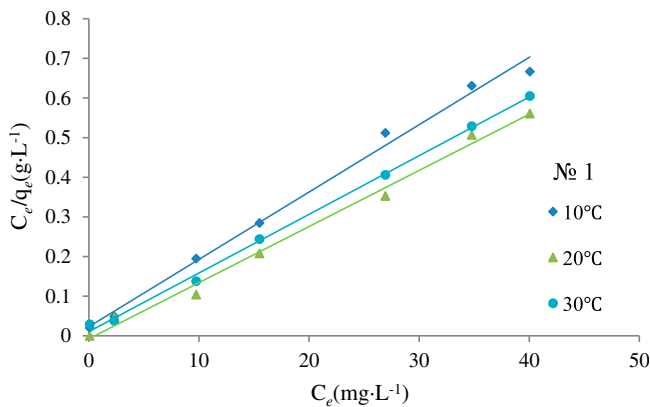


Fig. 8a. Fitting curve of Langmuir isotherm equation of X-3B on adsorbent No. 1.

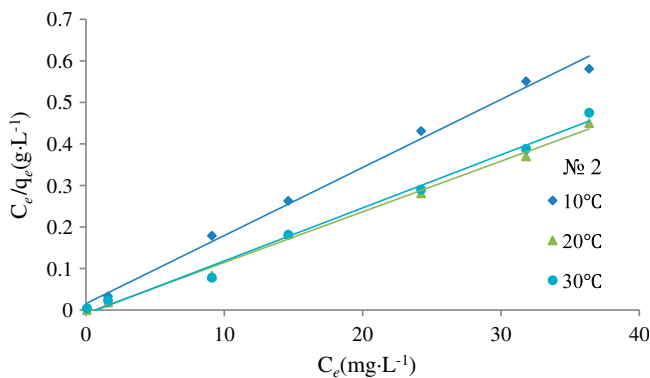


Fig. 8b. Fitting curve of Langmuir isotherm equation of X-3B on adsorbent No. 2.

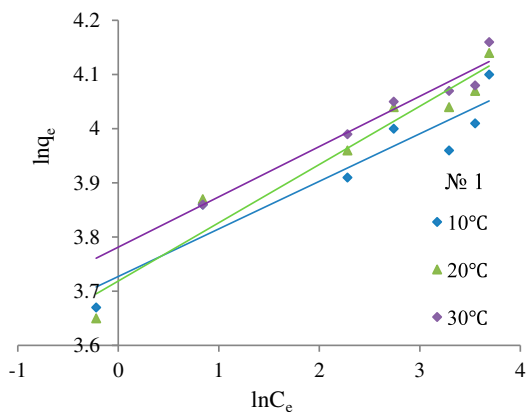


Fig. 8c. Fitting curve of Freundlich isotherm equation of X-3B on adsorbent No. 1.

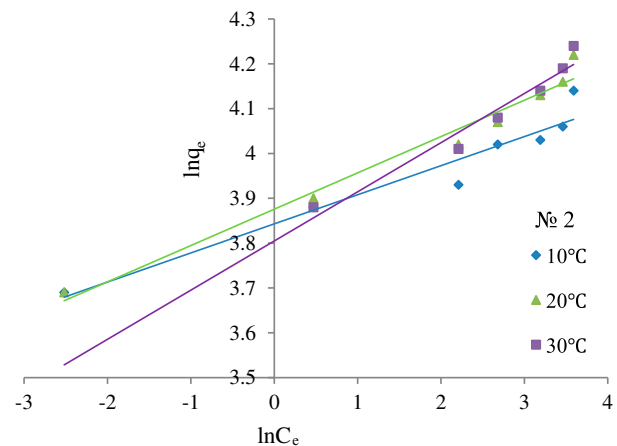


Fig. 8d. Fitting curve of Freundlich isotherm equation of X-3B on adsorbent No. 2.

empirical formula that describes equilibrium on heterogeneous surfaces; as a result, it does not assume monolayer capacity [29]. The model can be expressed as follows:

$$\ln q_e = \frac{1}{n} \ln C_e + \ln K_F \quad (6)$$

where  $K_F$  is the Freundlich constant, and  $1/n$  is the index of concentration.  $K_F$  and  $1/n$  are indicators of the adsorption capacity and adsorption intensity, respectively.  $1/n$  values between 0.1 and 0.5 represent good adsorption potential of the adsorbent.

The adsorption of X-3B was measured at 10, 20, and 30°C. The experimental data were fitted using Eqs. (5) and (6). The fitting equations are shown in Figs. 8a–8d. The parameters of fitting isothermal equations are shown in Table 4.

Seen from Figs. 8a–8d, and Table 4 shows that the Langmuir model apparently fits the adsorption better than the Freundlich model, given the correlation coefficient values ( $R^2$ ) of the former model are greater than those of the latter at the same temperature. In other words, the adsorption of X-3B can be categorized as monolayer adsorption.

Meanwhile, the Langmuir equation parameter  $Q_m$  changes with a change in temperature in both adsorbents No. 1 and No. 2, indicating that the adsorption of X-3B is an endothermal process, which is in accordance with previous studies [30].

X-3B is a reactive dye, and its activity can be influenced by temperature. Therefore, a moderately higher temperature favors the adsorption of X-3B.

Table 4  
Isotherm parameters for X-3B adsorption onto adsorbents No. 1 and No. 2

Isothermal models	Parameters	No. 1			No. 2		
		10°C	20°C	30°C	10°C	20°C	30°C
Langmuir	$Q_m$ (mg g <sup>-1</sup> )	58.82	62.11	62.89	60.98	67.57	68.97
	$b$ (L mg <sup>-1</sup> )	0.75	0.94	1.31	1.06	1.26	1.19
	$R^2$	0.9934	0.9967	0.9966	0.9939	0.9971	0.9957
Freundlich	$1/n$	0.0878	0.1075	0.0929	0.0649	0.081	0.1097
	$K_F$ (mg g <sup>-1</sup> (L mg <sup>-1</sup> ) <sup>1/n</sup> )	41.56	41.21	43.87	46.67	48.22	44.92
	$R^2$	0.8893	0.9438	0.9468	0.9397	0.9739	0.9502

Table 5  
Contents (mg kg<sup>-1</sup>) of Zn, Pb, Cr, Cd, Cu, Ni, Mn, and Fe in raw materials

Element	Zn	Pb	Cr	Cd	Cu	Ni	Mn	Fe
Content	3,460	330	140	12	45	97	118	66,200

Finally, the values of  $1/n$  in the Freundlich model are all between 0.1 and 0.5, indicating that it is easier to absorb X-3B from wastewater [3].

### 3.4. Heavy metal content of oily sludge and adsorbents

Various metals, especially heavy metals, such as Zn, Pb, Cr, Cu, Ni, and Fe, are present in oily sludge [31–33]. Moreover, the presence of Cd and Mn in the raw material is noted. The contents of the above-mentioned eight metals in the raw material are shown in Table 5.

Special attention has been given to the metals present in the adsorbents during the entire experiment. Two liquid samples and six other liquid samples (5 mL for each sample) were obtained after kinetic

and isothermal studies, respectively. The samples from the isothermal study were randomly obtained from each temperature and each adsorbent. The organics of these samples were degraded using nitric acid, and the metals in the processed samples were then detected. The results are shown in Table 6.

Table 6 shows that the leaks of the seven other metals from the adsorbent to the liquid are all less evident, whereas Fe is present in high concentrations in all the samples. The FTIR analysis shows that the lab-made adsorbents contain certain amounts of metallic oxide generated at high temperatures and therefore hardly dissolves in the X-3B solution. Iron is more active than other metals, given that its oxides and salts can dissolve in the acidic X-3B solution; hence, iron ions are present in the solution after adsorption at high concentrations.

### 3.5. Comparing with commercial AC

According to Dolas et al. [1] and Saygılı et al. [34], wooden AC can have a BET surface area ranging from 314 to 3,822 m<sup>2</sup> g<sup>-1</sup>, with a pore volume ranging from 0.03 to 4.59 cm<sup>3</sup> g<sup>-1</sup>. In our comparison experiment, the

Table 6  
Contents (mg kg<sup>-1</sup>) of Zn, Pb, Cr, Cd, Cu, Ni, Mn, and Fe in liquid samples taken after kinetic and isothermal studies, respectively

Element		Zn	Pb	Cr	Cd	Cu	Ni	Mn	Fe
Kinetic No. 1	20°C	1.97	0.10	0.28	–	0.12	0.09	0.03	69.12
Kinetic No. 2	20°C	1.92	0.08	0.25	–	0.13	0.07	0.04	67.35
Isothermal No. 1	10°C	4.10	0.18	0.15	–	0.34	0.08	0.05	13.18
	20°C	4.71	0.12	0.24	–	0.85	0.09	0.07	43.42
Isothermal No. 2	30°C	2.28	0.18	0.17	0.11	0.17	0.08	0.04	14.41
	10°C	2.38	0.17	0.18	0.12	0.74	0.10	0.05	21.48
	20°C	3.86	0.19	0.28	0.04	0.21	0.11	0.03	67.28
	30°C	2.54	0.16	0.21	0.05	0.19	0.07	0.08	48.35

Note: “–” represents the content of the element cannot be detected.

BET surface area and pore volume of the common commercial ACs are  $660 \text{ m}^2 \text{ g}^{-1}$  and  $0.09 \text{ cm}^3 \text{ g}^{-1}$ , respectively, with an adsorption equilibrium time of more than 17 h and an adsorption capacity of  $144 \text{ mg g}^{-1}$ . By contrast, the BET surface area and pore volume of the lab-made adsorbent are  $183 \text{ m}^2 \text{ g}^{-1}$  and  $0.19 \text{ cm}^3 \text{ g}^{-1}$ , respectively, with an adsorption equilibrium time of 8 h and an adsorption capacity of  $61 \text{ mg g}^{-1}$ . Moreover, the lab-made adsorbent and commercial AC have nearly the same adsorption capacity in the first 8 h. Considering the gap of the BET surface area, pore volume, and cost between the lab-made adsorbent and commercial AC, the adsorption results of oily sludge-made adsorbent are acceptable, although improvement is needed in future studies.

#### 4. Conclusion

Adsorbents were produced from oily sludge dewatered using Fenton's reagent and sawdust. The adsorbents that were carbonized at  $800^\circ\text{C}$  for 45 min with the  $\text{ZnCl}_2$  dosage of 40 wt% performed better than those carbonized at the temperature of  $700^\circ\text{C}$  in adsorbing X-3B, and the former adsorbent has a surface area of  $183 \text{ m}^2 \text{ g}^{-1}$  and a total volume of  $0.19 \text{ cm}^3 \text{ g}^{-1}$ .

The kinetic study indicates that the adsorption of X-3B on the adsorbent closely fits the pseudo-second order model. The isothermal study shows that the adsorption of X-3B is in accordance with the Langmuir model and can therefore be categorized as monolayer adsorption. The isothermal study also shows that the adsorption of X-3B is an endothermic process, given that the  $Q_m$  increases with an increase in temperature. The adsorbent which is carbonized at  $800^\circ\text{C}$  can have a maximum adsorption capacity of  $61 \text{ mg g}^{-1}$  at  $30^\circ\text{C}$  with an equilibrium time of 8 h.

A total of eight metals, including some heavy metals are detected in both the raw material and liquid gained after adsorption. The final result indicates that the leaking of heavy metals into the liquid is not evident, whereas Fe is more easily dissolves in the liquid.

Although the lab-made adsorbent has a weaker adsorption capacity than common commercial AC, its lower cost and adsorption equilibrium time can be an advantage. Furthermore, the production of adsorbent from dewatered oily sludge needs improvement to generate material with better properties.

#### Acknowledgments

The work was financially supported by the National Natural Science Foundation of China

(51208290). And the author thanks the Sixth Oil Exploiting Plant of Zhongyuan Oil Field and Huangtai Furniture Market for applying the raw oily sludge and sawdust, respectively. We are also grateful to CNGC Institute 53 for supplying facilities in our research.

#### References

- [1] H. Dolas, O. Sahin, C. Saka, H. Demir, A new method on producing high surface area activated carbon: The effect of salt on the surface area and the pore size distribution of activated carbon prepared from pistachio shell, *Chem. Eng. J.* 166 (2011) 191–197.
- [2] Q. Shi, J. Zhang, C. Zhang, W. Nie, B. Zhang, H. Zhang, Adsorption of Basic Violet 14 in aqueous solutions using  $\text{KMnO}_4$ -modified activated carbon, *J. Colloid Interface Sci.* 343 (2010) 188–193.
- [3] R. Xiaoli, Y. Ling, L. Min, Kinetic and thermodynamic studies of acid scarlet 3R adsorption onto low-cost adsorbent developed from sludge and straw, *Chin. J. Chem. Eng.* 22 (2014) 208–213.
- [4] M.A.A. Zaini, M. Zakaria, S.M. Setapar, M. Che-Yunus, Sludge-adsorbents from palm oil mill effluent for methylene blue removal, *J. Environ. Chem. Eng.* 1 (2013) 1091–1098.
- [5] E. Siswoyo, Y. Mihara, S. Tanaka, Determination of key components and adsorption capacity of a low cost adsorbent based on sludge of drinking water treatment plant to adsorb cadmium ion in water, *Appl. Clay Sci.* 97–98 (2014) 146–152.
- [6] L.J. da Silva, F.C. Alves, F.P. de Franca, A review of the technological solutions for the treatment of oily sludges from petroleum refineries, *Waste Manage. Res.* 30 (2012) 1016–1030.
- [7] G. Hu, J. Li, G. Zeng, Recent development in the treatment of oily sludge from petroleum industry: A review, *J. Hazard. Mater.* 261 (2013) 470–490.
- [8] S. Guo, G. Li, J. Qu, X. Liu, Improvement of acidification on dewaterability of oily sludge from flotation, *Chem. Eng. J.* 168 (2011) 746–751.
- [9] M. Kriipsalu, M. Marques, D.R. Nammari, W. Hogland, Bio-treatment of oily sludge: The contribution of amendment material to the content of target contaminants, and the biodegradation dynamics, *J. Hazard. Mater.* 148 (2007) 616–622.
- [10] T. Basegio, F. Berutti, A. Bernardes, C.P. Bergmann, Environmental and technical aspects of the utilisation of tannery sludge as a raw material for clay products, *J. Eur. Ceram. Soc.* 22 (2002) 2251–2259.
- [11] M. Kriipsalu, M. Marques, A. Maastik, Characterization of oily sludge from a wastewater treatment plant flocculation–flotation unit in a petroleum refinery and its treatment implications, *J. Mater. Cycles Waste Manage.* 10 (2008) 79–86.
- [12] B. Pinheiro, J. Holanda, Obtainment of porcelain floor tiles added with petroleum oily sludge, *Ceram. Int.* 39 (2013) 57–63.
- [13] M. Xu, J. Zhang, H. Liu, H. Zhao, W. Li, The resource utilization of oily sludge by co-gasification with coal, *Fuel* 126 (2014) 55–61.
- [14] X. Long, G. Zhang, C. Shen, G. Sun, R. Wang, L. Yin, Q. Meng, Application of rhamnolipid as a novel

- biodemulsifier for destabilizing waste crude oil, *Bioresour. Technol.* 131 (2013) 1–5.
- [15] C. Zhang, S. Yang, H. Chen, H. He, C. Sun, Adsorption behavior and mechanism of reactive brilliant red X-3B in aqueous solution over three kinds of hydrotalcite-like LDHs, *Appl. Surf. Sci.* 301 (2014) 329–337.
- [16] G. Xu, Y. Zhang, G. Li, Degradation of azo dye active brilliant red X-3B by composite ferrate solution, *J. Hazard. Mater.* 161 (2009) 1299–1305.
- [17] J. Xu, Y. Ao, D. Fu, C. Yuan, Study on photocatalytic performance and degradation kinetics of X-3B with lanthanide-modified titanium dioxide under solar and UV illumination, *J. Hazard. Mater.* 164 (2009) 762–768.
- [18] X. Zhang, G. Li, Y. Wang, Microwave assisted photocatalytic degradation of high concentration azo dye Reactive Brilliant Red X-3B with microwave electrodeless lamp as light source, *Dyes Pigm.* 74 (2007) 536–544.
- [19] X. Fang, J. Xiao, S. Yang, H. He, C. Sun, Investigation on microwave absorbing properties of loaded  $\text{MnFe}_2\text{O}_4$  and degradation of Reactive Brilliant Red X-3B, *Appl. Catal. B: Environ.* 162 (2015) 544–550.
- [20] X. Wu, D. Wu, R. Fu, Studies on the adsorption of reactive brilliant red X-3B dye on organic and carbon aerogels, *J. Hazard. Mater.* 147 (2007) 1028–1036.
- [21] H. Guo, S. Feng, J. Jiang, M. Zhang, H. Lin, X. Zhou, Application of Fenton's reagent combined with sawdust on the dewaterability of oily sludge, *Environ. Sci. Pollut. Res.* 21 (2014) 10706–10712.
- [22] X. Wang, J. Jia, Y. Wang, Enhanced photocatalytic-electrolytic degradation of Reactive Brilliant Red X-3B in the presence of water jet cavitation, *Ultrason. Sonochem.* 23 (2015) 93–99.
- [23] Y. Kan, Q. Yue, J. Kong, B. Gao, Q. Li, The application of activated carbon produced from waste printed circuit boards (PCBs) by  $\text{H}_3\text{PO}_4$  and steam activation for the removal of malachite green, *Chem. Eng. J.* 260 (2015) 541–549.
- [24] A.L. Cazetta, A.M. Vargas, E.M. Nogami, M.H. Kunita, M.R. Guilherme, A.C. Martins, T.L. Silva, J.C. Moraes, V.C. Almeida, NaOH-activated carbon of high surface area produced from coconut shell: Kinetics and equilibrium studies from the methylene blue adsorption, *Chem. Eng. J.* 174 (2011) 117–125.
- [25] A.C. Martins, O. Pezoti, A.L. Cazetta, K.C. Bedin, D.A. Yamazaki, G.F. Bandoch, T. Asefa, J.V. Visentainer, V.C. Almeida, Removal of tetracycline by NaOH-activated carbon produced from macadamia nut shells: Kinetic and equilibrium studies, *Chem. Eng. J.* 260 (2015) 291–299.
- [26] Z. Li, Q. Tang, T. Katsumi, X. Tang, T. Inui, S. Imaizumi, Leaf char: An alternative adsorbent for Cr(III), *Desalination* 264 (2010) 70–77.
- [27] I. Velghe, R. Carleer, J. Yperman, S. Schreurs, J. D'Haen, Characterisation of adsorbents prepared by pyrolysis of sludge and sludge/disposal filter cake mix, *Water Res.* 46 (2012) 2783–2794.
- [28] I. Langmuir, The adsorption of gases on plane surfaces of glass, mica and platinum, *J. Am. Chem. Soc.* 40 (1918) 1361–1403.
- [29] H. Freundlich, Adsorption in solution, *WJ Helle, J. Am. Chem. Soc.* 61 (1939) 2–28.
- [30] M.M. Rahman, N. Akter, M.R. Karim, N. Ahmad, M.M. Rahman, I. Siddiquey, N.M. Bahadur, M. Hasnat, Optimization, kinetic and thermodynamic studies for removal of Brilliant Red (X-3B) using Tannin gel, *J. Environ. Chem. Eng.* 2 (2014) 76–83.
- [31] T. Roldán-Carrillo, G. Castorena-Cortés, I. Zapata-Peñasco, J. Reyes-Avila, P. Olguín-Lora, Aerobic biodegradation of sludge with high hydrocarbon content generated by a Mexican natural gas processing facility, *J. Environ. Manage.* 95 (2012) S93–S98.
- [32] O.R.S. da Rocha, R.F. Dantas, M.M.M.B. Duarte, M.M.L. Duarte, V.L. da Silva, Oil sludge treatment by photocatalysis applying black and white light, *Chem. Eng. J.* 157 (2010) 80–85.
- [33] J.A. Marín, J.L. Moreno, T. Hernández, C. García, Bioremediation by composting of heavy oil refinery sludge in semiarid conditions, *Biodegradation* 17 (2006) 251–261.
- [34] H. Saygılı, F. Güzel, Y. Önal, Conversion of grape industrial processing waste to activated carbon sorbent and its performance in cationic and anionic dyes adsorption, *J. Clean. Prod.* 93 (2015) 84–93.